Indirect Measurements of Added-wave Resistance On an In-service Container Ship

Ulrik D. Nielsen[1,4], Jacob R. Johannesen[2], Harry B. Bingham[1], Mogens Blanke[1,5], and Soizic Joncquez[3]

[1] Technical University of Denmark, Kgs. Lyngby DK-2800, Denmark
[2] DFDS, Copenhagen DK-2100, Denmark
[3] Maersk Line, Copenhagen DK-1098, Denmark
[4] NTNU AMOS, Trondheim NO-7491, Norway
[5] Propeller Control ApS, Kgs. Lyngby DK-2800, Denmark

Abstract. This paper investigates a semi-empirical model used to estimate added-wave resistance on a ship sailing in waves. The model relies on measurements from a continuous monitoring system, and produces an estimate - the indirect measurement - of added-wave resistance, based on the difference between, on the one side, the measured power and, on the other side, a summation of theoretically calculated resistance contributions but neglecting the component because of seaway. Hence, the added-wave power is obtained as the surplus. The model has been applied to more than three months of full-scale data recorded on an in-service operating container ship. The results indicate reasonable levels of the added-wave power, emphasising that both positive and negative values are obtained, since the model is *not* restricted to relative wave directions forward of beam. It is found that following waves often lead to 'negative resistance', in fact creating a thrust, but, importantly, following waves can also increase the total resistance significantly.

Keywords: Added-wave resistance, indirect measurements, continuous monitoring system, following waves, correction procedures

1 Introduction

The estimation of added-wave resistance on a ship sailing in waves has received increased interest since slow steaming became the common practice of merchant ships some years ago. The increasing interest relates to the fact that added-wave resistance plays a more significant role, relative to the other resistance components, when vessel forward speed is reduced. In the larger picture, the estimation of added-wave resistance has its importance in relation to energy efficiency and environmentally friendly shipping. In the same context, as a consequence of regulations aimed at reducing installed engine power, the associated risk of designing under-powered ships is of key importance [25].

This paper presents a study focused on a method to indirectly measure added-wave resistance using full-scale data from a sailing ship. The indirect measurement is based on a semi-empirical model using a combination of, on the one

side, measurements of engine power, and, on the other side, operational data to estimate all significant resistance components acting on the sailing vessel *except* the added-wave resistance. Testing has been performed with measurements from an in-service operating container vessel. It is noteworthy that the particular approach has a clear resemblance to 'correction procedures' developed to remove or correct for external factors such as wind, waves, etc., when modelling resistance of ships in connection with sea trials [8, 9, 17, 18, 26, 37].

The available literature about performance monitoring and general resistance modelling using experimental, in-service data has increased significantly in recent years, e.g. [1, 23, 31, 38, 39]. In particular, conferences such as HullPIC and COMPIT have attracted a lot of studies. In addition to the aforementioned references about added-wave resistance and performance monitoring, some interesting (subjective) thoughts/opinions are presented in [6]. Herein, numerical approaches to estimate added-wave resistance in seaways are reviewed, and [6] concludes that "*Added resistance is difficult to predict, regardless what approach is taken, especially in short or oblique waves*". Furthermore, it is stated that "*Accurate models for added power in waves make only sense if also more accurate data for the ambient seaway is obtained*". In this view, it makes sense to (in)directly measure the added-wave resistance from an approach that does not need information about the 'ambient seaway', and neither does the model rely on theoretical modelling of added-wave resistance.

2 Resistance On a Ship Sailing In Waves

The resistance (force) exerted on a ship sailing in waves is the sum of the calm-water resistance and a number of "extra" contributions, denoted collectively as the *added resistance*. Among the latter is the additional resistance component resulting because of *seaway* and the interactions between waves and ship; in the paper this component is referred to as the *added-wave resistance*. Next to the added-wave resistance, the additional resistance components of the semi-empirical model are: Wind resistance, resistance due to rudder action, and shallow water effects. Other resistance components exist but they will not be considered herein. In the following, some general remarks are given about the considered resistance components, including the calm-water resistance, but all details and calculation formulas are given in the literature.

2.1 Calm-water Resistance

For a given (full-scale) ship, it is common practice to calculate the magnitude of the full-scale resistance force by use of model-scale experimental tests, as suggested in the ITTC-1978 Method, e.g. [16]. In the present study, the full-scale calm-water resistance is estimated from previously conducted model tests, including resistance tests, open water tests, and self-propulsion tests; all with a mounted rudder and thruster tunnel bores in the hull. The calculation of the calm-water resistance thus becomes a matter of making interpolation in a set

of speed-power curves (applicable in full-scale), depending on actual values of draught and speed. It is noteworthy that alternative methods can be applied to estimate the calm-water resistance, if towing tank tests are not available, e.g. [12, 15].

2.2 Wind Resistance

The wind resistance depends on the relative wind speed and direction, and the projected windage area of the ship. Wind tunnel tests can be introduced for calculating/extrapolating the wind resistance on a ship in full-scale. On the other hand, if wind tunnel tests are *not* available, as the case is in the present study, [11] has proposed a numerical estimation model, based on extensive experimental investigations, for the wind resistance on container vessels. The details of the model are given by [11], but it proves useful to consult also [41] because of its tabulated values of coefficients and parameters used in the model.

2.3 Resistance Due to Rudder Action

Wind (and waves) may also create a net force in the direction perpendicular to ship's centreline and, together with a yawing moment, this necessitates rudder actions to maintain the intended straight-line course. The application of a non-neutral rudder angle initiates a transverse force and a steering moment about the centre of gravity of the ship by deflecting the water flow to the direction of the water plane of the rudder profile. Consequently, rudder actions give rise to an increase in the longitudinal resistance on the ship, and herein modelling is made by use of [4, 21].

2.4 Shallow Water Effects

The overall consequence of shallow water, in relation to resistance calculations, has been quantified by [22, 33]. The former of the two has been widely used in industry. However, the numerical results presented later are based on the (corrected) estimate from [32], due to its applicability for a wider range of speed-to-depth ratios and less conservative results as compared to the other model [22].

2.5 Added-wave Resistance

Although the added-wave resistance is not theoretically modelled, since it is 'measured', a few remarks should be included. As pointed out in the literature, e.g. [5, 14, 20, 34, 43], added-wave resistance is typically explained as a result of three phenomena: (a) *Wave reflection*; i.e. diffraction, of the incident waves by the ship. The energy for this diffraction is associated with an increase in resistance. (b) *Ship motions*; in particular, the vertical motions heave and pitch have the largest effect. This "component" is due to the damping force from the motions of the vessel when the water is calm. (c) *Interference* between incident

waves and waves generated by the ship when heaving and pitching, sometimes referred to as 'drift'.

It is well-known that theoretical calculations of added-wave resistance have several complications and complexities connected to them. In fact, this is the main reason to establish an estimate based on indirect measurements instead.

3 Indirect Measurements of Added-wave Resistance

The resistance contributions making up the total resistance on a sailing ship in waves have been described in the previous section. Explicit calculation formulas for all contributions, except for the added-wave resistance, have been implemented in a numerical model. The model is semi-empirical as the single resistance components in their theoretical formulations rely on parameters that can, or *must*, be measured. For the analysed example ship, see Section 4, the necessary measurements are all available through auto-logged data from a continuous monitoring system. This section presents the basic concept of the numerical (and semi-empirical) model.

3.1 Equilibrium Between Resistance and Thrust

As a ship moves forward at constant speed, there is a balance between the propulsive force F_T and the total resistance R_{tot} where $F_T = (1-t)T$ with t being the thrust deduction factor and T the augment of the total required thrust (at the tailshaft). In the study, it is assumed that the total resistance includes all contributions, except the added-wave resistance R_{AW}, and, assuming a steady-state equilibrium between (effective) thrust and resistance, the following formula holds:

$$0 = F_T - (R^*_{tot} + R_{AW}) \tag{1}$$

where $R^*_{tot} + R_{AW} = R_{tot}$. The equation considers a 'steady-state' condition taking operational data (e.g. vessel forward speed, heading, main engine power) and environmental data (e.g. sea state, wind, water depth, sea temperature) as constant within the measurement period. In the semi-empirical model, "samples" of operational data is based on average-calculations considering 3-minutes periods evenly distributed around discrete time stamps coinciding, or synchronised, with samples of environmental (hindcast) data every 30-minutes. Additional information about the sensors is included in Section 4.

3.2 Relation Between (Total) Resistance and Engine Power

The thrust on a vessel corresponds to an effective power P_E,

$$P_E = F_T \cdot V = R_{tot} \cdot V \tag{2}$$

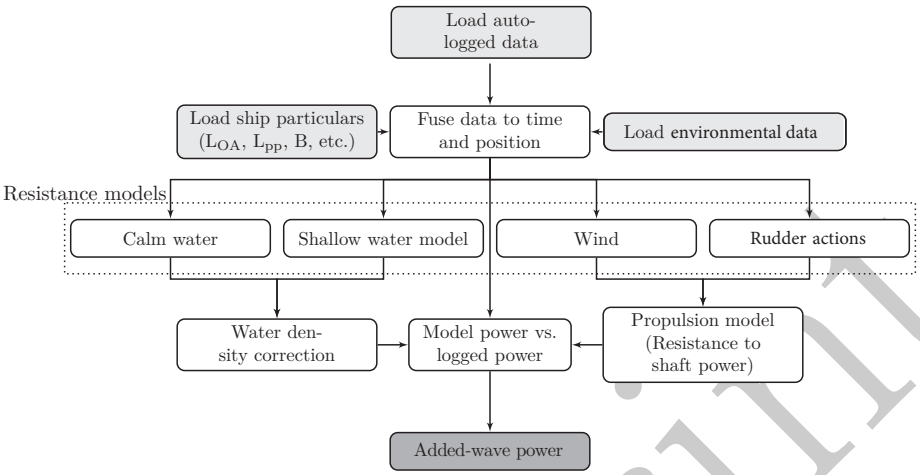

Fig. 1. Flow-chart to arrive at an estimate of the added-wave resistance, equivalently added-wave power. The diagram applies to post-voyage processing

where V is the ship's (constant) speed-through-water (STW). The total efficiency $\eta_{tot} = \eta_H \times \eta_O \times \eta_R \times \eta_S$ of the propulsion system is a product between the hull efficiency (η_H), the open-water efficiency (η_O), the relative rotative efficiency (η_R), and the shaft efficiency (η_S), e.g. [13, 24]. Based on the total efficiency, it is possible to estimate the necessary shaft power (or brake power) P_S, to be generated by the machinery (i.e. main engine), for a required effective power P_E. In fact, the "direction" is the opposite; meaning that measurements of generated engine power P_S are converted to an effective power by taking into account the total efficiency of the propulsion system. The estimate of the *total* resistance is therefore given by, cf. Eq. (2),

$$R_{tot} \cdot V = P_S \cdot \eta_{tot} \tag{3}$$

and, together with the semi-empirical result for R^*_{tot}, it is possible to obtain an indirect measurement of the added-wave resistance,

$$R_{AW} = \frac{P_S}{V} \cdot \eta_{tot} - R^*_{tot} \tag{4}$$

The semi-empirical approach has been implemented in MATLAB®, and a graphical illustration of the model is presented in Figure 1 that applies for post-voyage conditions. It is noteworthy that the modelled resistance components are converted to shaft power components. Accordingly, the outcome of the semi-empirical model is (required) *added-wave power* instead of added-wave resistance. In the diagram, see Figure 1, the load of 'environmental data' includes hindcast data used to validate the auto-logged data. In this study, the analysis is made as a post-voyage process but, in principle, the analysis could run real-time

and be presented to the ship master and to the on-shore vessel performance analysis team; emphasising that all necessary measurements are available from the continuous monitoring system installed on the vessel, while the hindcast data is used solely for validation purposes.

As a practical remark, in this paper there is no distinguishing between (readings of) *main engine power* and *shaft power*, since the case ship is equipped with a directly-coupled two stroke main engine. The two terms may therefore be used interchangeably, which would not be the case if, say, a medium-sized engine with a gearbox had been installed.

3.3 Assumptions About Propulsive Coefficients

The propulsive efficiency of a ship is highly affected by the propulsion coefficients. Thus, the wake fraction coefficient w and the thrust deduction factor t are important for an accurate estimate of the propulsion force, which in turn is used to estimate the added-wave resistance in the present indirect, or inverse, approach. In this study, it is assumed that the propulsion coefficients are constant and independent of the actual seaway and sailing conditions (in a time-averaged sense), although it is known that waves and wave-induced motions can lead to variations as studied by, e.g. [35,36]. The assumption about constant propulsion coefficients may be somewhat justified, exactly because the analysis builds on 3-minutes time-averaged sensor readings, cf. Subsection 4.1. Irrespectively the (potential) violation of constant propulsive coefficients, any further investigations in this direction are beyond the scope of the present study.

4 Example Ship and Sensor Installations

The case ship is a 7,200 TEU container vessel. The vessel's main particulars are listed in Table 1.

Table 1. Main particulars of the example ship.

Length between perpendiculars, L_{pp}	332 m
Breadth moulded, B_m	42.8 m
Design draught, T_d	12.2 m
Deadweight (at T_d),	76,660 tonnes
Block coefficient, C_B	0.65

4.1 Data Acquisition and Filtering

The layout of the example ship's sensor installations is sketched in Figure 2. The measurements from the sensors are auto-logged by a central data logging

system. The relevant sensors to this study are listed in Table 2 that includes sample frequencies and ranges. Note that data from the auto-logging system is available every 10th second, hence SF = 0.1 Hz, which (probably) represents a mean value over the past 10 seconds from the raw sensor signals. However, the exact details of this (averaging) "re-sampling technique" are not known to the authors.

Table 2. Sensor specifications: Sampling frequency (SF), acquisition range, and unit.

Type	SF	Range	Unit
GPS Time Stamp	0.1 Hz	-	-
Lattitude	0.1 Hz	-90 - 90	deg
Longitude	0.1 Hz	-180 - 180	deg
Shaft Speed	0.1 Hz	-100 - 100	RPM
Shaft Torque	0.1 Hz	0 - 7500	kNm
Longitudinal STW	0.1 Hz	0 - 60	knots
Transverse STW	0.1 Hz	0 - 60	knots
GPS SOG	0.1 Hz	0 - 30	m/s
Rudder angle	0.1 Hz	-35 - 35	deg
Ship heading	0.1 Hz	0 - 360	deg
Rel. Wind Direction	0.1 Hz	0 - 360	deg
Rel. Wind Speed	0.1 Hz	- 100 - 100	knots
Draught Aft	0.1 Hz	0 - 100	m
Draught Fore	0.1 Hz	0 - 100	m
Water Depth (below keel)	0.1 Hz	0 - 10,000	m

The auto-logged data was collected while the ship was in service along the route sketched in Figure 3. Specifically, measurements have been collected during roughly 3 months. For the exact analysis, the measurements were filtered for erroneous samples and, subsequently, consideration has been given to data corresponding to approximately 3,800 'discrete' 3-minutes average-samples separated by 30 minutes, see Subsection 3.1. In addition to erroneous samples, the data

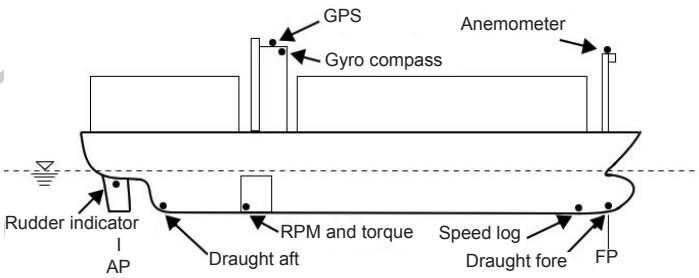

Fig. 2. Illustration of sensors and their locations.

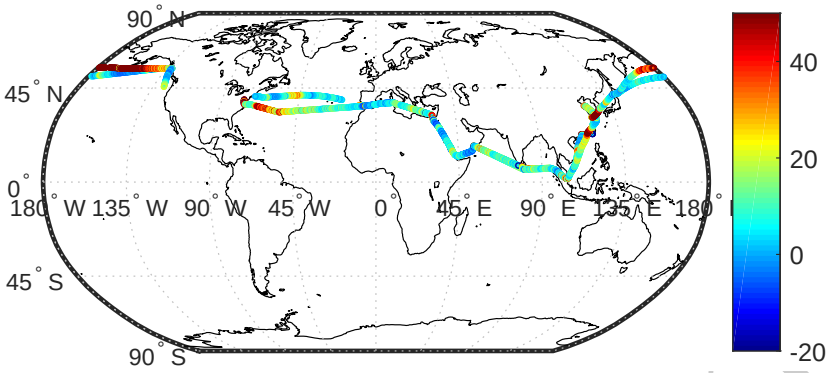

Fig. 3. Vessel route and logged main engine power. The coloured map (in percentages) of power reflects the relative difference between actual power measurements and corresponding (theoretical) power estimates in calm water; noting that a percentage smaller than 0% represents power measurements of less than what would be required in case of calm-water conditions. Some measurements exceed the colour scale, but, in this case, data is coloured according the upper/lower limits (50%/-20%).

was filtered to keep only measurements with a speed of more than 10 knots. It is noteworthy, see Figure 3, that the logged main engine power in several occasions was less than what, theoretically, would be required in an otherwise calm-water for identical operational conditions.

5 Results and Discussions

5.1 Pre-evaluation of Measurement Conditions

Hindcast Wave Data As indicated previously, hindcast wave data - obtained from an external provider - has been fused into the auto-logged data, since information about the sea state is useful for investigative purposes, although the information is not required for the model to run. Results for significant wave height H_s, zero-upcrossing period T_z, and wave heading β are shown in Figure 4; $\beta = 180$ deg. is head seas. The main observation from Figure 4 is that the wave conditions were fairly mild during most of the measurement campaign, although severer conditions did occur around the middle part and towards the end of the data stream.

In the remaining parts of the paper the hindcast wave data is considered *accurate*. In reality, however, the analysis and measuring of sea states, even through hindcast studies, can be associated with (large) uncertainty. The authors have *not* attempted to further study the validity of the hindcast wave data itself.

Operational Data Next to having information about the wave conditions it is useful to study some of the operational parameters during the measurement

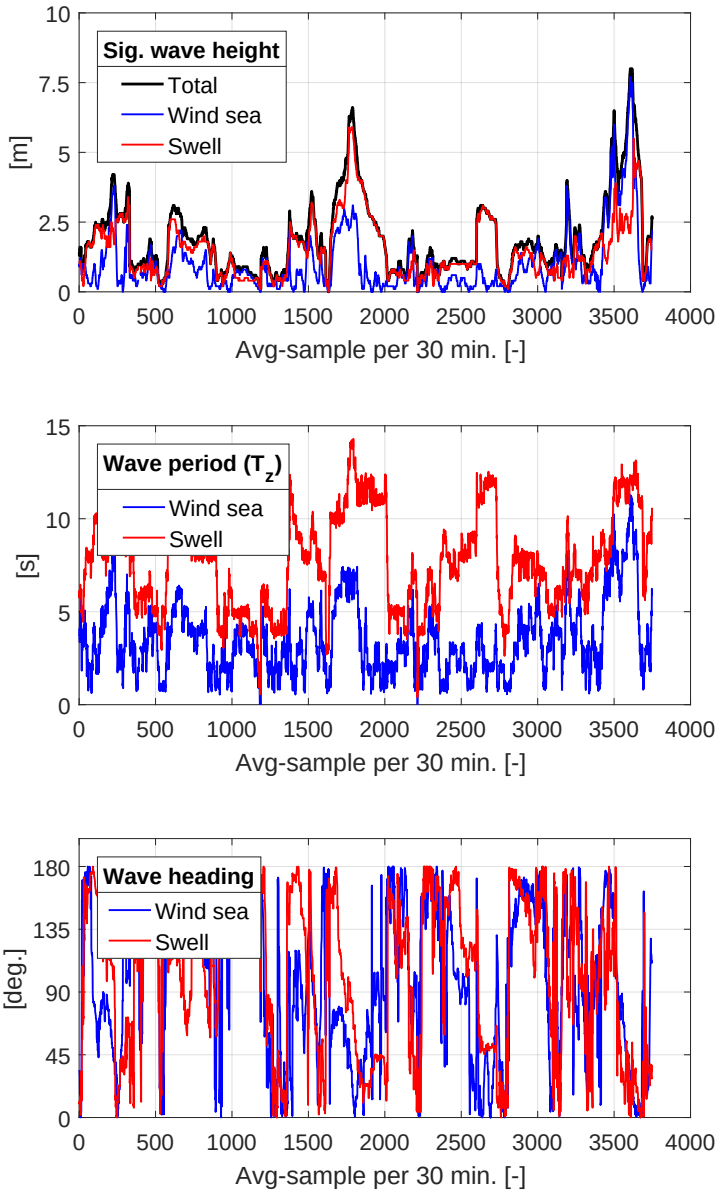

Fig. 4. Significant wave height, H_s (top), zero-upcrossing wave period, T_z (middle), and wave heading β (bottom) as obtained from hindcast data. The horizontal axis represents 3-minutes average-samples separated by 30 minutes. Note that abrupt changes may be the result of discontinuous data, cf. Subsection 4.1.

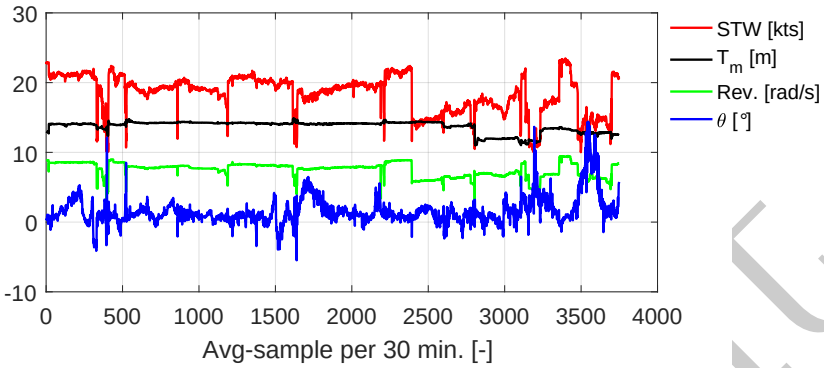

Fig. 5. Operational parameters.

period. Figure 5 shows measurements of logged speed-through-water (STW), shaft revolutions per second (Rev.) corresponding to RPM, mean draught (T_m), and the rudder angle (θ). From the figure it is interesting to see how STW is reduced and, at the same time, how rudder movement increases during the more severe wave conditions in the middle part and, notably, at the end of the data stream.

It is seen that several 'spikes' occur in the measurements (in STW, RPM, and rudder angle), but these are not signs of faulty or untrustworthy data; instead they are reflections of a change in loading condition in connection with ports of call.

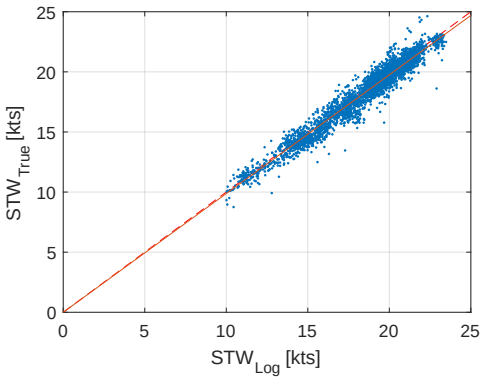

Fig. 6. Logged speed-through-water versus "true" speed-through-water. It can be seen that the best linear fit (full red line) is almost coinciding with the dashed red line representing identity between logged and true values.

The credibility of the *logged* STW, by the Doppler Velocity Log (DVL), is often discussed and questioned, e.g. [3,30]. In the present investigation, however, there is little indication that the logged STW should be particularly untrustworthy. This can be seen from Figure 6, where the logged STW is mapped together with the "true" STW, based on the vessel's speed-over-ground (from GPS) and sea current (from hindcast); although several individual cases are off, the general picture is reasonable.

Main Finding The pre-evaluation of the measurement conditions, including environmental and operational data, indicates that the required input to the semi-empirical model for calculating the added-wave resistance generally is considered to be of sufficient quality and fairly trustworthy.

5.2 Semi-empirical Estimation of Added-wave Power

The estimate of the added-wave power depends on measurements of the main engine power (MEP) and the calculated resistance contributions, cf. Sections 2 and 3. Figure 7 presents the individual contributions of the analysis, noting that the *modelled* resistance components all are given as corresponding 'shaft powers'. Generally, the modelled calm-water resistance is dominant but wind is also significant, whereas the effect of steering and drift (rudder) is almost vanishing. For the shallow water contribution, a few spurious cases exist, where the water depth data exceeds the limitations of the shallow water model as given by [32].

Based on the semi-empirical model, the added-wave power is obtained from Eq. (4), and the result is shown in Figure 8 emphasising that the result reflects the estimated added-wave power normalised with the MEP.

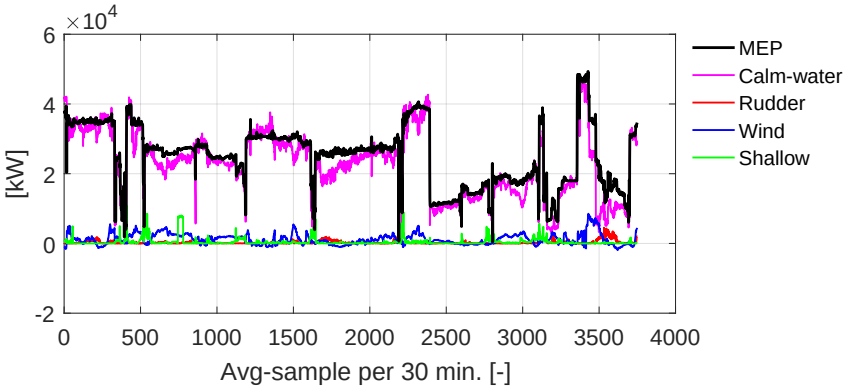

Fig. 7. Measurements of MEP and modelled resistance components converted into corresponding 'shaft power contributions'.

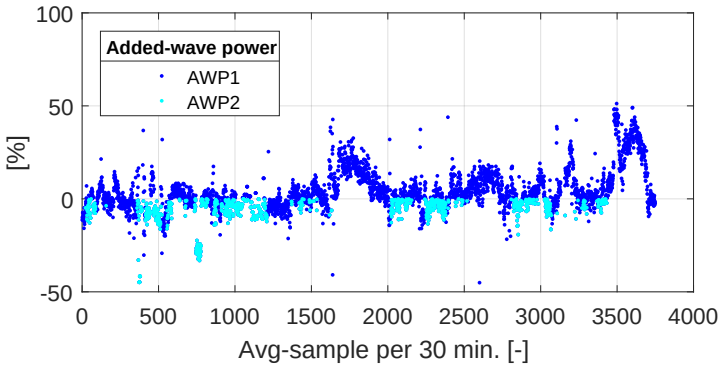

Fig. 8. Added-wave power normalised by main engine power (MEP). The trustworthy results are indicated by 'AWP1', while 'AWP2' represents erroneous results.

As the first observation, it is noted that both positive and negative values of the added-wave power occur. In itself, negative values are not a conflicting observation for a ship sailing in *following* waves[1] according to other experimental studies [19, 42]. However, with complete trust in the hindcast wave data, some of the negative values actually occur while the ship has been operating in head sea conditions, including both wind sea and swell. In this case, the particular negative results are erroneous, since head sea conditions must always lead to an increase in the total resistance. In the plot, see Figure 8, the erroneous results are marked as 'AWP2'. Hence, under the assumption of truly accurate hindcast wave data, only the blue curve-segments, marked as 'AWP1', can be considered as trustworthy *indirect measurements* of the added-wave power. The trustworthy results of the added-wave power have been redrawn in a separate plot, as shown in Figure 9, where the added-wave power is given in dimensional form in kW. The black and red horizontal line segments indicate conditions of following waves, i.e. $\beta \in [0°, 90°[$, where the black segments represent that either the wind sea *or* the swell part (if present) was creating following waves, while the red segments correspond to following waves created by *both* the wind sea and the swell part (if present). Consequently, *negative* added-wave power can appear *just* on the parts indicated by a black or red line, while the opposite is not true; the ship may certainly feel (positive) added-wave resistance, even in following wave conditions.

With an exclusive focus on the blue curve-segments in Figure 8, and the equivalent plot in Figure 9, the following observations should be noted: (1) Negative added-wave power occurs; however, the occurrences are confirmed to appear just when the ship operates in following waves, where the added-wave 'resistance' from a theoretically point-of-view *can* be negative but *may* also be positive(!).

[1] In the present discussion, the term *head sea conditions* refers to $\beta \in [90°, 180°]$, while *following waves* covers everything with $\beta \in [0°, 90°[$.

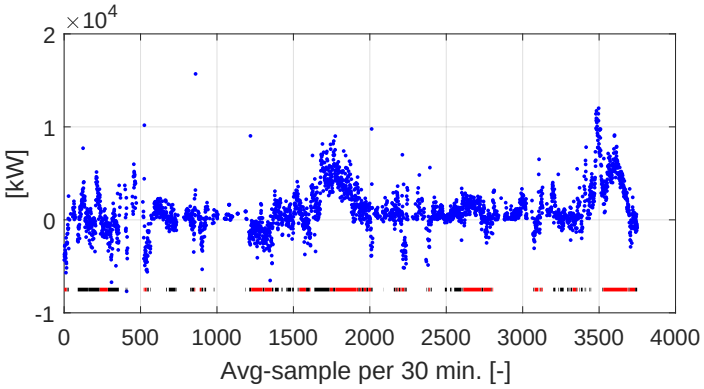

Fig. 9. Added-wave power in dimensional form and filtered for results "confirmed" as erroneous. The black and red horizontal line segments represent conditions with following waves.

(2) A number of "unreliable" spikes occur in the results, positive as well as negative. However, the spikes can be referred to as cases with sudden changes in the operational parameters, cf. Figure 5, and it was previously discussed that these abrupt variations were simply a result of ports of call. (3) The *indirect measurements* of added-wave power reveal that, for the set of measurements, the resistance because of seaway may take a share of up to 8-12 MW or approximately 40-50 % of the total power in some cases. It is no surprise to see that the particular cases are reflected by the largest wave heights, cf. Figure 4. (4) Interestingly, in the middle and latter parts of the data stream, where the largest wave heights occur, see also (3), the wave headings were *not* head sea but, in fact, represented by following wave conditions with $\beta \in [0° - 90°[$, cf. Figures 4 and 9. This observation underlines the complexity in dealing with added-wave resistance on ships sailing in real seaway. As a supplementary note, it has been investigated if the wave heading *really* was reflected by following waves, like the hindcast wave data reveals. It is therefore noteworthy that the wind resistance on the ship, during the questioned periods, is negative, see Figure 7, which means that tail winds occur; confirming that *at least* the wind sea part of the wave system do represent following waves. It has not been possible to confirm the direction of the swells, but it is believed that the hindcast data is reliable, for what reason the particular periods (indicated by red horizontal lines in Fig. 9) really were conditions with following waves.

5.3 Credibility and General Discussions

The presented results indicate reasonable levels of the added-wave resistance. Nevertheless, the credibility of the results is relevant to discuss and to indicate reasons ("effects") that could imply inaccurate estimates; also because no comparative measures have been included in the analysis. Generally, the accuracy of

the added-wave resistance model is governed by limitations in the sub-models, cf. Section 2, together with faults and errors in the auto-logged data which is input to the sub-models:

- The implemented calm-water resistance model is based on an interpolation scheme between the vessel's draught and its speed-through-water (STW). The draught measurement is believed to be fairly accurate as opposed to the STW obtained from the speed log (Doppler Velocity Log). A study of the STW measurements showed inaccuracies in the individual cases but, on average, the measurements were reasonable. Nonetheless, as power depends on speed raised to a power of (approximately) 3, even small errors can be damaging for the result.
- The data implemented in the wind model has been found to be accurate by comparison to hindcast data (although not shown in the paper). The wind model, however, suffers from the fact that it is based on an average container stack configuration [2].
- The rudder model is based on the linearised assumption of small rudder angles. This assumption is appropriate in open sea conditions where only small rudder corrections normally are applied but for maneuvering conditions the assumption breaks down.
- The 'shallow water resistance problem' has the fundamental limitation that no model is valid for very shallow waters.

It has not been attempted to implement all resistance contributions in the model. Effects of fouling on hull and propeller should be included to obtain a more accurate model. Exclusion of the hull fouling is assessed to result in a constant relative offset in model results, as the considered time period is limited (about three months). The effect of fouling on the propeller is also expected to affect the model significantly, as the consequence is lowered propeller open water efficiency and larger shaft power measurements than the model estimates. Furthermore, the effect of trim has not been included in the model as it is difficult to make an empirical estimate of this effect. Finally, the case ship, cf. Section 4, is equipped with retractable fins, but their usage is not logged during operations at sea. Therefore, the effect of stabilisers has not been included in the resistance estimation.

In the study, hindcast wave data was used for validation purposes. In fact, parts of the results relating to estimates of the added-wave resistance were considered erroneous, since the indirect measurements in the particular cases showed negative values; even though the vessel, according to the hindcast data, was operating in head sea conditions. It must be stressed, however, that hindcast wave data is itself often prone to errors, and, therefore, it may be that the *true* wave heading not necessarily represents head seas ($\beta \in [90^\circ - 180^\circ]$). On the other hand, in the given cases, (relative) wind measurements indicate (true) wind directions that correspond to wave directions resulting in head sea conditions; at least for the wind waves. Any further discussion on this topic is left as future work.

The propulsion coefficients were assumed to be constant, with the wake fraction coefficient and the thrust deduction factor determined for one particular condition independent of the seaway and the wave-induced motions of the ship. Relatively few researches have explored the fact that, in reality, the propulsion coefficients vary [10,36,40]. In further studies, it should be attempted to properly model the variation of the propulsion factors to improve the indirect approach for obtaining estimates of added-wave resistance. For the particular ship and the data studied in the present paper, however, the effect of variations in the propulsion coefficients is negligible. This has been tested in a small sensitivity study based on results where the thrust deduction factor and the wake fraction coefficient have been modelled as stochastic variables. In the sensitivity study, the coefficients were modelled as being log-normal distributed around a mean value and with standard deviation equal to 20% of the mean value. The mean values of the two coefficients were set identical to the values used in the previous analyses where the coefficients were constant. Thus, Monte Carlo simulation has been used to study the sensitivity of variations in the propulsion factors, and, based on 1,000 simulations at each 30-minutes measurement sample, the outcome is as shown in Figure 10. In the figure, the blue dots are identical to the results from Figure 9, while the black curves represent the result of the 1,000 simulations. Consequently, as the 1,000 black curves are mapped (nearly) on top of each other, it is seen that the effect of variations in the propulsion coefficients is insignificant in this particular case. However, it is important to note that this result cannot be generalised, since different findings may be revealed, depending on the ship and propulsion system, as has also been reported by [35].

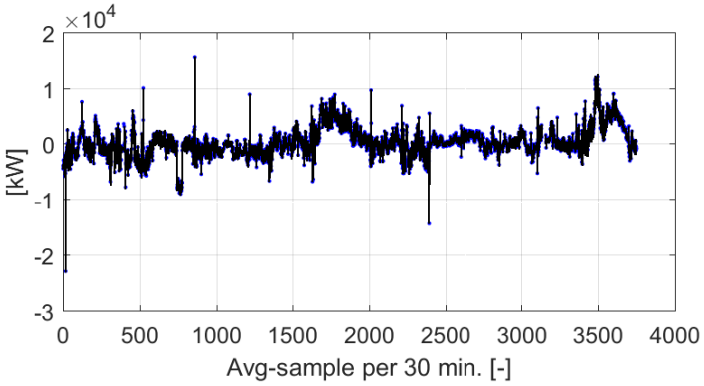

Fig. 10. Added-wave power with stochastic modelling of propulsion coefficients (black curves) and with constant propulsion coefficients (blue dots).

6 Summary and Conclusions

A semi-empirical approach to estimate added-wave resistance based on auto-logged onboard measurements has been developed. The approach provides *indirect measurements* of the added-wave resistance by combining measurements of the main engine power and other input data used for modelling/calculating all relevant resistance contributions, *except* the added-wave resistance. The difference between the modelled resistance, or equivalently power, and the actual measured power represents the effect of added resistance due to seaway.

Generally, the added wave resistance model seems to give reasonable results, with the neglect of (confirmed) erroneous results. For some operational conditions the estimated added-wave resistance accounted for about 50 % of the total measured power. As opposed to other conventional theoretical added-wave resistance methods, the developed method also considers the effect of following sea conditions, including everything from following waves to beam waves, and the possibility of negative values for the same. It was observed that following waves imply 'negative' resistance contributions in many cases, but, adding to the complexity of studies about added-wave resistance, it was found that following waves, in severe conditions, may very well lead to a significant increase in the total resistance on the ship. As a related note, the fact that seaway in itself sometimes lead to a thrust (negative resistance), or more generally a varying load on the propeller, is reflected by studies looking into optimising the propeller shaft speed, e.g. [7].

6.1 Further Work

First and foremost, validation of the *indirect measurements* of the added-wave resistance should be attempted; for instance, by comparison with numerical calculations based on theoretical works and associated computational tools. Secondly, it should be interesting to implement a procedure for sea state estimation, e.g. the wave buoy analogy [27–29], to allow for estimates of the wave conditions exactly where the ship is. Such an implementation would inherently lead to analyses of the motion recordings of the ship, and this type of analysis would in itself be interesting as a complement to the semi-empirical model for added-wave resistance, since the findings from the analysis of the wave-induced motions can be used to improve the estimate of added-wave resistance.

For the actual model, as discussed in the paper, it would be beneficial to include results from hull condition reports to determine the effect of fouling. Besides, the developed model will benefit by adding trim condition corrections to the results, which could be achieved by including data from trim optimisation towing tests or from CFD simulations. Moreover, it is recommended to improve the wind model by including data on the container stack configuration, realising that results are sensitive hereto, especially for oblique wind conditions.

Acknowledgement

The authors would like to acknowledge that data was collected by Propeller Control ApS and Maersk A/S through the Blue Innoship Project 2, which was supported by the Danish Innovations Fund, the industrial partners and the Danish Maritime Fund. The work by the first author has been supported by the Research Council of Norway through the Centres of Excellence funding scheme, Project number 223254-AMOS.

References

1. Adland, R., Cariou, P., Jia, H., Wolff, F.C.: The energy efficiency effects of periodic ship hull cleaning. Journal of Cleaner Production **178** (2018) 1–13
2. Andersen, I.: Wind loads on post-panamax container ship. Ocean Engineering **58** (2013) 115–134
3. Antola, M., Solonen, A., Pyorre, J.: Notorious Speed Through Water. In: Proc. of 2nd Hull Performance and Insight Conference, Ulrichshusen, Germany (2017)
4. Aoki, I., Kijima, K., Nakiri, Y., Fukuwara, Y.: On the prediction method for maneuverability of a full scale ship. J. Japan S. of Naval Arch. and Ocean Engineers **3** (2006) 157–165
5. Arribas, F.: Some methods to obtain the added resistance of a ship advancing in waves. Ocean Engineering **34** (2007) 946–955
6. Bertram, V.: Added Power in Waves Time to Stop Lying (to Ourselves). In: Proceedings of 1st HullPIC Confence, Castello di Pavone, Italy (2016) 5–13
7. Blanke, M., Pivano, L., Johansen, T.: An Efficiency Optimizing Shaft Speed Control for Ships in Moderate Seas. IFAC Proceedings Volumes (CAMS Conference) **40** (2007) 329–336
8. British Standard: ISO 15016: Ships and marine technology - Guidelines for the assessment of speed and power performance by analysis of speed trial data. BSI Standards Limited (2015)
9. British Standard: ISO 19030: Ships and marine technology - Measurement of changes in hull and propeller performance. BSI Standards Limited (2016)
10. Faltinsen, O., Minsaas, K., Liapis, N., Skjørdal, S.: Prediction of resistance and propulsion of a ship in a seaway. In: Proc. 13th Symposium on Naval Hydrodynamics, Tokyo, Japan (1980)
11. Fujiwara, T., Tsukada, Y., Kitamura, F., Sawada, H., Ohmatsu, S.: Experimental investigation and estimation on wind forces for a container ship. In: Proc. 19th ISOPE, Osaka, Japan (2009)
12. Guldhammer, H., Harvald, S.: Ship Resistance - The effect of form and principal dimensions. Akademisk Forlag (1970)
13. Harvald, S.: Resistance and Propulsion of Ships. John Wiley (1983)
14. Havelock, T.: Drifting Force on a Ship among Waves. Philosophical Magazine **33** (1942) 467–475
15. Holtrop, J., Mennen, G.: An approximate power prediction method. J. Intl. Shipbuilding Progress **29** (1982) 166–170
16. ITTC: 1978 ITTC Performance Prediction Method. Technical report, International Towing Tank Conference, Rio de Janeiro, Brazil (2011)

17. ITTC: Analysis of speed/power trial data. Recommended Procedures and Guidelines. Technical report, 27th International Towing Tank Conference, Copenhagen, Denmark (2014)
18. ITTC: Preparation, conduct and analysis of speed/power trial data. Recommended Procedures and Guidelines. Technical report, 28th International Towing Tank Conference, Wuxi, China (2017)
19. Journée, J.: Motions and Resistance of a Ship in Regular Following Waves. Technical report, Delft University of Technology, Ship Hydromechanics Laboratory, Delft, The Netherlands (1976)
20. Journée, J., Massie, W.: Offshore Hydromechanics (January 2001) Lecture notes in course offered at TU Delft.
21. Kijima, K., Katsuno, T., Nakiri, Y., Fukuwara, Y.: On the maneuvering performance of a ship with the parameter of loading condition. J. Japan S. of Naval Arch. and Ocean Engineers **168** (1990) 141–148
22. Lackenby, H.: The effect of shallow water on ship speed. Shipbuilder and Marine Engine Builder **76** (1964) 21–26
23. Lu, R., Turan, O., Boulougouris, E., Banks, C., Incecik, A.: A semi-empirical ship operational performance prediction model for voyage optimization towards energy efficient shipping. Ocean Engineering **110** (2015) 18–28
24. MAN Energy Solutions: Basic Principles of Ship Propulsion. MAN (2018) Available online: www.man-es.com.
25. Marine Environment Protection Committee: Guidelines for determining minimum propulsion power to maintain the manoeuvrability of ships in adverse conditions. IMO Circular MEPC 71/INF.29, International Maritime Organization, London, UK (2017)
26. Molland, A., Turnock, S., Hudson, D.: Ship Resistance and Propulsion. Cambridge University Press (2011)
27. Nielsen, U.D.: Estimations of on-site directional wave spectra from measured ship responses. Marine Structures **19** (2006) 33–69
28. Nielsen, U.D.: A concise account of techniques available for shipboard sea state estimation. Ocean Engineering **129** (2017) 352–362
29. Nielsen, U.D., Brodtkorb, A.H., Sørensen, A.J.: A brute-force spectral approach for wave estimation using measured vessel motions. Marine Structures **60** (2018) 101–121
30. Oikonomakis, A., Galeazzi, R., Dietz, J., Nielsen, U., Holst, K.: Application of Sensor Fusion to Drive Vessel Performance. In: Proc. of 4th Hull Performance and Insight Conference, Gubbio, Italy (2019)
31. Orihara, H., Tsujimoto, M.: Performance prediction of full-scale ship and analysis by means of on-board monitoring. Part 2: Validation of full-scale performance predictions in actual seas. Journal of Marine Science and Technology **23** (2018) 782–801
32. Raven, H.: A new correction procedure for shallow-water effects in ship speed trials. In: Proc. 13th PRADS, Copenhagen, Denmark (2016)
33. Schlichting, O.: Schiffswiderstand auf beschränkter Wassertiefe - Widerstand von Seeschiffen auf flachem Wasser (in German). STG Jahrbuch **35** (1934)
34. Ström-Tejsen, J., Yeh, H., Moran, D.: Added resistance in waves. Trans. SNAME **81** (1973) 109–143
35. Taskar, B., Regener, P., Andersen, P.: The impact of propulsion factors on vessel performance in waves. In: Proc. of 6th Intl. Symp. on Marine Propulsors, Rome, Italy (2019)

36. Taskar, B., Yum, K., Steen, S., Pedersen, E.: The effect of waves on engine-propeller dynamics and propulsion performance of ships. Ocean Engineering **122** (2016) 262–277
37. Telfer, E.: The practical analysis of merchant ship trials and service performance. Trans North East Coast Inst Eng Shipbuild **43** (1926) 63–98
38. Trodden, D., Murphy, A., Pazouki, K., Sargeant, J.: Fuel usage data analysis for efficient shipping operations. Ocean Engineering **110** (2015) 75–84
39. Tsujimoto, M., Orihara, H.: Performance prediction of full-scale ship and analysis by means of onboard monitoring (Part 1 ship performance prediction in actual seas). Journal of Marine Science and Technology **Accessed online** (2018) 1–18
40. Ueno, M., Tsukada, Y., Tanizawa, K.: Estimation and prediction of effective inflow velocityto propeller in waves. Journal of Geophysical Research **18** (2013) 339–348
41. Ueno, T.F.M., Ikeda, Y.: A new estimation method of wind forces and moments acting on ships on the basis of physical component methods (in Japanese). J. Japan S. of Naval Arch. and Ocean Engineers **2** (2005) 243–255
42. Valanto, P., Hong, Y.: Experimental Investigation on Ship Wave Added Resistance in Regular Head, Oblique, Beam, and Following Waves. In: Proc. 25th ISOPE, Kona, HI, USA (2015)
43. Wilson, P.: A review of the methods of calculation of added resistance for ships in a seaway. Journal of Wind Engineering and Industrial Aerodynamics **20** (1985) 187–199